Supporting Information for

Estimating Marine Carbon Uptake in the Northeast Pacific Using a Neural Network Approach

Patrick J. Duke[1], Roberta C. Hamme[1], Debby Ianson[2,1], Peter Landschützer[3], Mohamed M. M. Ahmed[1,4], Neil C. Swart[5,1], Paul A. Covert[2]

[1]School of Earth and Ocean Sciences, University of Victoria, Victoria, BC, Canada
[2]Institute of Ocean Sciences, Fisheries and Oceans Canada, Sidney, BC, Canada
[3]Flanders Marine Institute (VLIZ), Ostend, Belgium
[4]Education and Research Group, Esri Canada, Calgary, AB, Canada
[5]Canadian Centre for Climate Modelling and Analysis, Environment and Climate Change Canada, Victoria, BC, Canada

Correspondence to: P. J. Duke (pjduke@ucalgary.ca)

Contents of this file

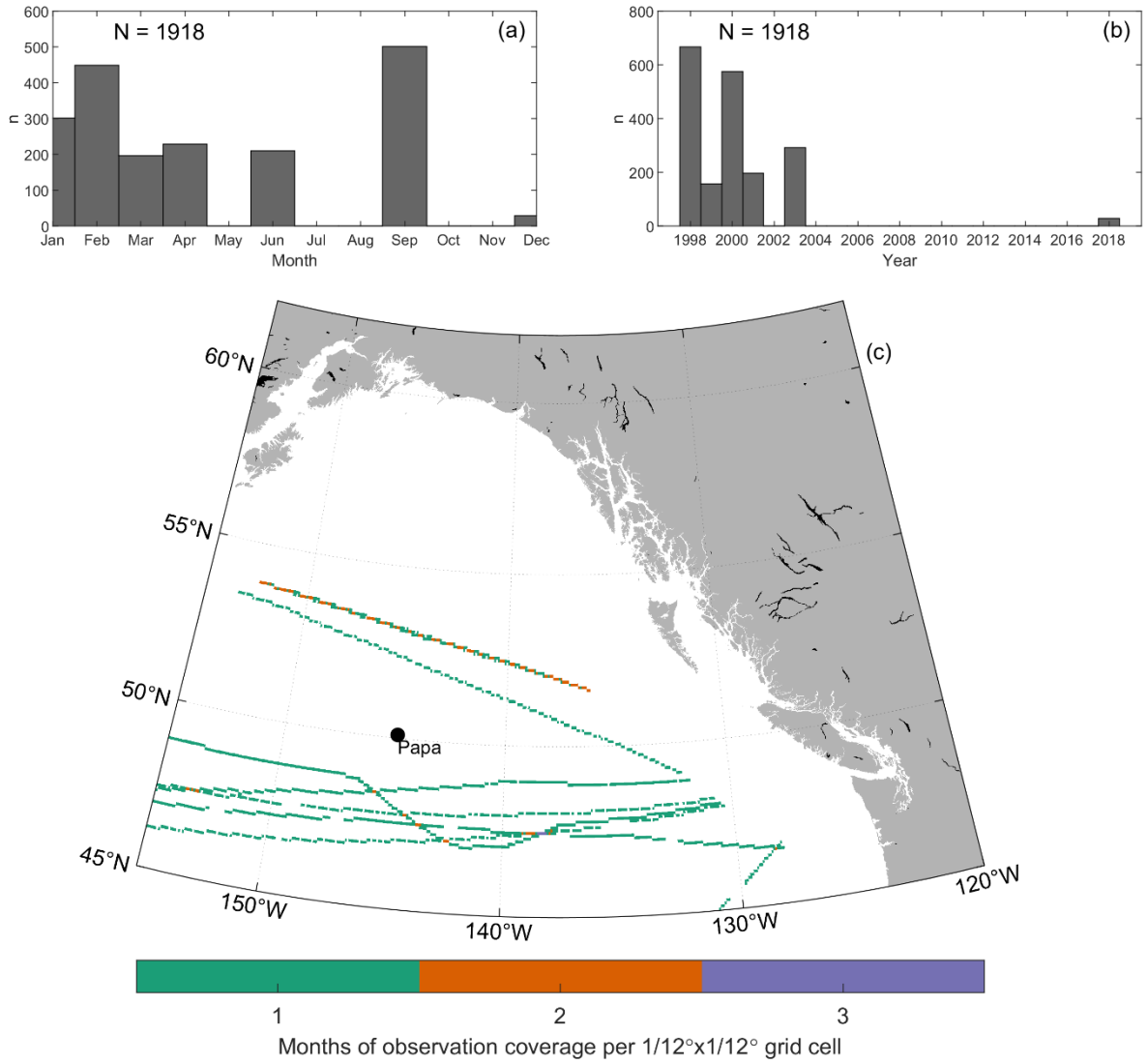

Figure S1 Withheld data distribution in (a) month, (b) years, (c) geographically as the number of months of observational coverage per 1/12°x1/12° grid cell. Ocean Station Papa is shown for reference.

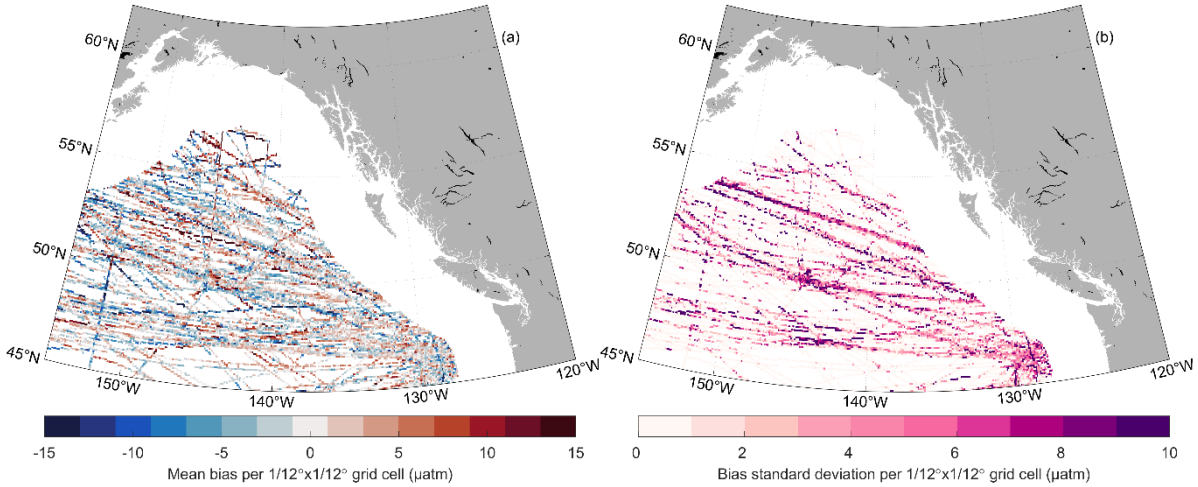

Figure S2 Mapped mean bias and standard deviation in residuals between ANN-NEP pCO_2 estimate and 1/12°x1/12° gridded SOCAT data.

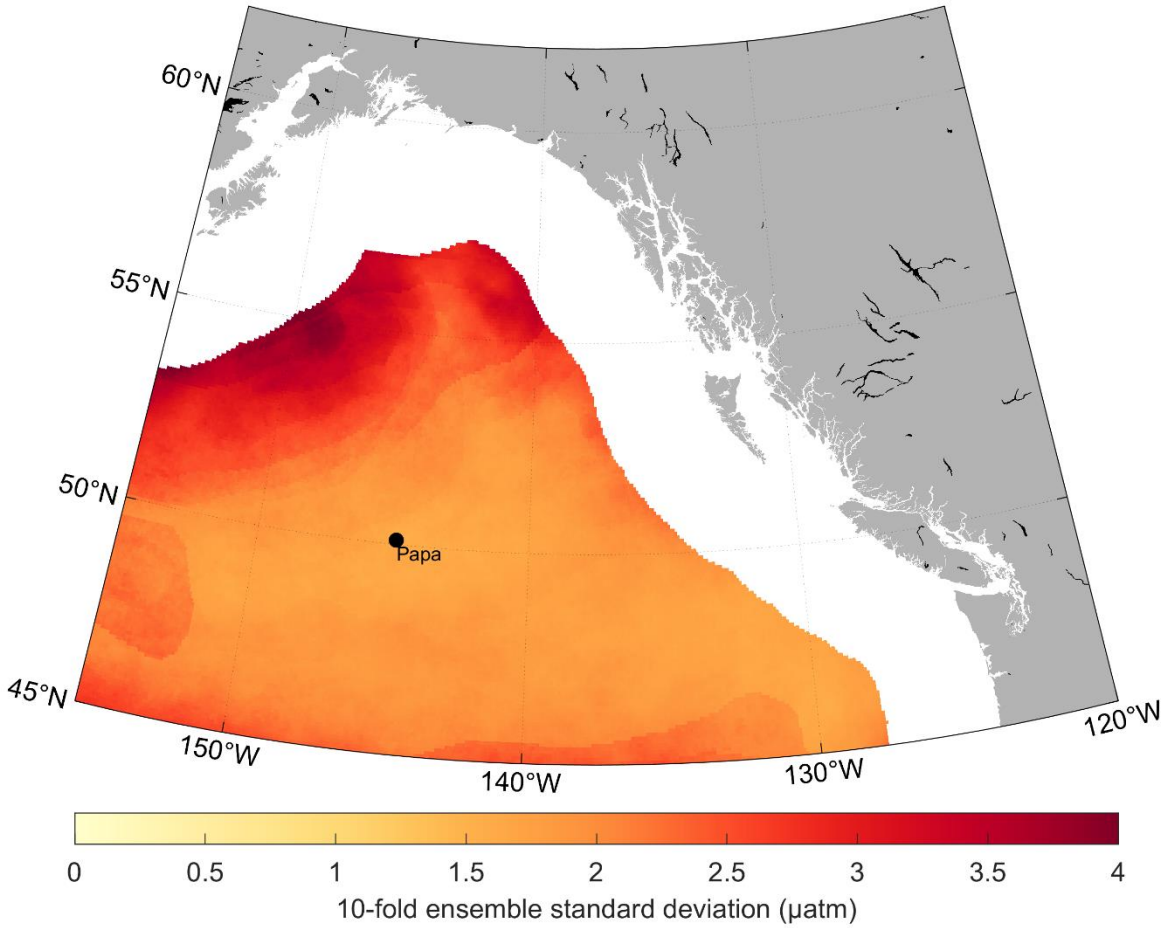

Figure S3 Mean pCO_2 standard deviation between ANN-NEP 10-fold ensemble members. Ocean Station Papa is shown for reference.

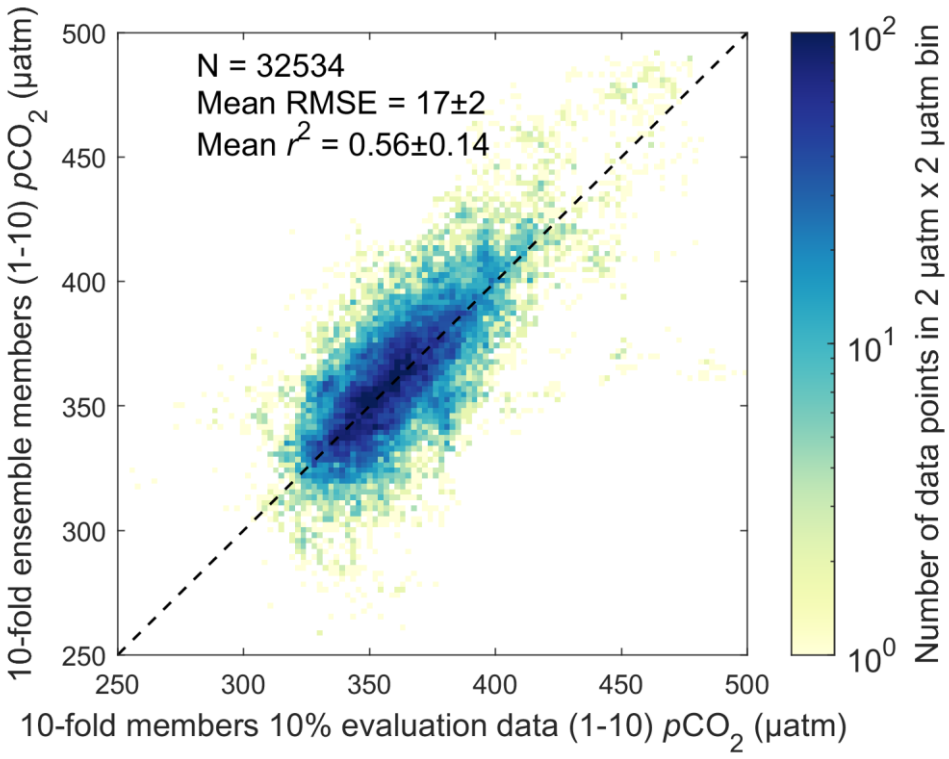

Figure S4 10-fold cross-evaluation (Section 2.4) individual ensemble member estimated pCO_2 against the 10% 10-fold evaluation data specific to that ensemble member. Mean root mean squared error (RMSE) and coefficient of determination (r^2) are across all individual ensemble members compared to the 10% evaluation data specific to that ensemble member. Data is binned into 2 µatm by 2 µatm bins. The dashed black line represents a perfect fit of slope (c_1) = 1 and intercept = 0.

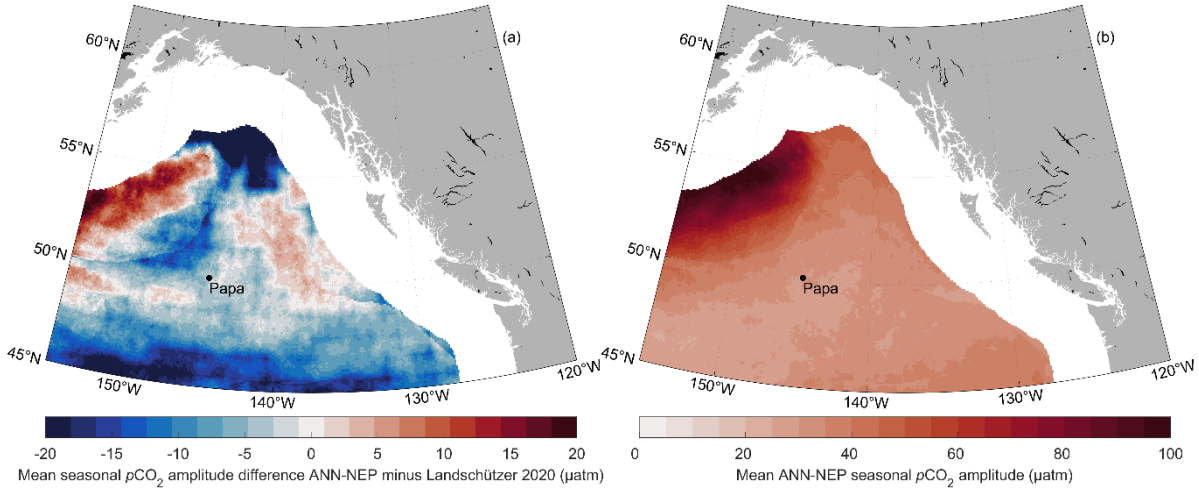

Figure S5 (a) Mean difference in the surface ocean pCO_2 seasonal amplitude in µatm between the ANN-NEP estimate (this study) and the Landschützer et al. (2020) global product. Positive (negative) differences indicate higher pCO_2 seasonal amplitude for the ANN-NEP (Landschützer et al. (2020)) estimate. The Landschützer et al. (2020) estimates have been interpolated to the

1/12°x1/12° grid of this study. (b) Mean ANN-NEP seasonal surface ocean pCO_2 seasonal amplitude in µatm. Ocean Station Papa is shown for reference.

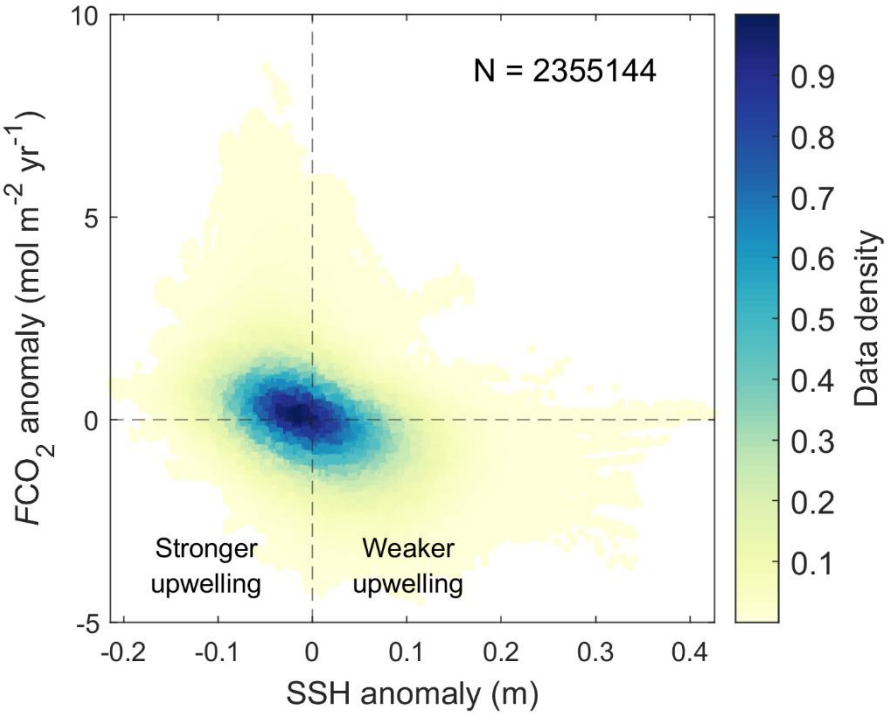

Figure S6 Property to property plot of air-sea CO_2 flux density anomalies and sea surface height (SSH) anomalies (grid cell by grid cell) in the subpolar Alaskan Gyre region of our study area (latitudes north of 52° N). Stronger (weaker) upwelling label relates to gyre upwelling strength driven by winds enhancing (damping) Ekman pumping and depressing (elevating) SSH.

Table S1 Regional high-resolution artificial neural network Northeast Pacific (ANN-NEP) pCO_2 product performance against all SOCAT pCO_2 observation data grouped by year and month. Number of observations (N), root mean squared error (RMSE), coefficient of determination (r^2), and mean bias (calculated as the mean residual).

	N	**RMSE**	r^2	**Mean bias**
Year				
1998	3085	8.1	0.73	-1.4
1999	2184	7.5	0.91	1.4
2000	5195	8.1	0.93	0.0
2001	2404	5.7	0.96	1.2
2002	2110	7.1	0.91	1.0
2003	2526	5.2	0.84	-1.3
2004	652	4.5	0.94	1.2
2005	110	6.8	0.69	-3.6
2006	413	3.3	0.93	-2.6
2007	405	6.4	0.87	-2.8
2008	217	4.0	0.95	-1.3
2009	2751	5.0	0.94	-0.4
2010	1267	6.5	0.96	1.9
2011	980	9.1	0.87	-1.0
2012	1567	6.1	0.93	1.3
2013	1593	4.3	0.99	0.9
2014	1017	5.1	0.95	-1.5
2015	836	9.1	0.95	1.5
2016	919	6.3	0.91	-0.4
2017	511	4.7	0.89	1.0
2018	1303	5.7	0.94	1.2
2019	2051	8.1	0.93	-0.6
Month				
January	2731	5.2	0.97	0.7
February	2971	5.8	0.98	-0.7

March	1816	6.8	0.96	-1.0
April	2277	4.3	0.97	0.3
May	3041	5.6	0.94	0.1
June	4077	9.0	0.92	-1.1
July	3601	9.6	0.86	-0.1
August	3922	7.5	0.94	1.0
September	4121	6.6	0.93	0.2
October	2240	4.9	0.91	1.2
November	1511	3.9	0.97	-0.4
December	1788	4.4	0.97	0.8

Table S2 Regional artificial neural network Northeast Pacific pCO_2 product performance at varying resolutions against training and independent withheld SOCAT pCO_2 observations. Mean and standard deviation between lower 10th percentile (5 of 50 runs) of overfitting metric values for each resolution with varying internal data division ratios between the pCO_2 training data used by the ANN to train and internally evaluate. Number of observations (N), root mean squared error (RMSE), coefficient of determination (r^2), mean absolute error (MAE), mean bias (calculated as the mean residual), and the slope of the linear regression (c_1). Courser resolution product uncertainties are also included where overall pCO_2 product uncertainty (θ_{pCO2}) is calculated from the square root of the sum of the three squared errors: observational uncertainty (θ_{obs}), gridding uncertainty (θ_{grid}), and ANN interpolation uncertainty (θ_{map}). The 10-fold ensemble approach was not run for the courser resolution products, likely leading to a slight underestimate of overall uncertainty as ANN run randomness uncertainty (θ_{run}) was excluded.

	Training data					
Resolution	**N**	**RMSE**	***r*^{2}**	**Mean Bias**	**c_1**	**MAE**
1°	2547	11.8±0.6	0.79±0.02	-0.1±0.1	0.73±0.02	8.8±0.5
1/2°	5569	10.9±0.7	0.83±0.02	0.1±0.2	0.77±0.02	7.9±0.6
1/4°	11253	11.3±0.9	0.82±0.03	0.0±0.1	0.77±0.03	8.2±0.7
1/8°	21869	12.2±1.0	0.79±0.03	0.0±0.2	0.74±0.03	8.8±0.8
1/12°	31392	10.5±1.0	0.84±0.03	0.0±0.2	0.79±0.03	7.4±0.8
	Independent withheld data					
1°	155	11.7±0.3	0.76±0.01	-0.7±0.5	0.88±0.01	8.4±0.1
1/2°	350	11.5±0.6	0.78±0.02	0.1±0.7	0.93±0.03	8.3±0. 5
1/4°	716	11.5±0.8	0.79±0.03	0.1±0.6	0.98±0.02	8.6±0. 7
1/8°	1387	12.5±0.6	0.76±0.01	-0.1±1.2	0.93±0.04	9.2±0. 5
1/12°	1857	11.4±0.5	0.79±0.01	2.1±0.6	0.92±0.03	8.4±0. 5
	pCO_2 product uncertainty					
	θ_{obs}	θ_{grid}	θ_{map}	θ_{pCO2}		
1°	3.1	3.7	11.7	12.6		
1/2°	3.1	2.8	11.5	12.3		
1/4°	3.1	2.0	11.5	12.2		
1/8°	3.1	2.0	12.5	13.0		